Research article

Research on setting method of fatigue warning sign on desert expressway based on driver's heart and myoelectric index

Xingang Wang [a], Xiangyun Hu [b,*], Xingli Jia [b], Zexuan Jiao [b]

[a] *Shaanxi Xigongyuan Engineering Testing Co., Ltd., Xi'an, China*
[b] *School of Highway Chang'an University, Xi'an, China*

A R T I C L E   I N F O

A B S T R A C T

Drivers are more likely to feel fatigue when driving on the desert highway due to its single line, monotonous road side landscape, and small traffic volume, etc., so the method of setting fatigue warning signs on desert highway should be studied for. In this paper, field investigation and field test are carried out on the section of Uma Expressway crossing Tengger Desert, and the same road scene and line shape as the actual one are constructed by using uc-win road. Driving simulation experiments were carried out by using driving simulation cabin, collecting heart and muscle electric indexes and analyzing fatigue characteristic law. On this basis, simulation experiments of different fatigue warning signs and stimulation intervals were carried out in multiple groups, and the pattern of cardiac and electromyographic indexes and the interaction law were analyzed based on the artifact correction method after denoising the measured data, so that the optimal setting method was obtained according to the stimulation effect. Based on the artifact correction method, the measured data were de-noised and analyzed the changes of ECG and EMG indexes and the interaction law, and the best setting method was obtained according to the stimulation effect. Finally, the fatigue level was classified based on the cohesive hierarchical system cluster analysis method to verify the rationality of the fatigue warning sign setting scheme. The results show that the driver's psychological fatigue and physiological fatigue both show obvious fluctuation growth, and the growth trend exists in four stages, namely, smooth fluctuation (0–30min), initial fatigue (35–85min), adjustment stage (85–160min), and severe fatigue (after 160min), and psychological fatigue is earlier than physiological fatigue, and the driver's regulation effect on physiological fatigue is better than psychological fatigue. Analysis of the psychological indexes of the four groups of traffic signs shows that the fatigue warning signs with black characters on a white background and set at an interval of 60–80 km have the most obvious effect on driver stimulation in a desert highway with a design speed of 80–100 km/h.

1. Introduction

At the current juncture, research endeavors pertaining to road traffic safety in desert regions primarily concentrate on exploring desert road alignment methodologies and the optimal placement of driver rest areas, with a preponderance of these studies centering on low-grade desert roads.Investigations have underscored the pervasive influence of human negligence, with traffic safety factors stemming from human oversight accounting for the lion's share of contributory elements. It has been shown that human negligence is

* Corresponding author.
  E-mail addresses: 1799290759@qq.com, 2022221319@chd.edu.cn (X. Hu).

the largest factor in all the factors affecting traffic safety.A notable void exists in research examining the specific impacts of desert environments on drivers and the performance of desert highways, as highlighted by Liu, Q. L. Zhang, and Y.B. Zou [1] in 2006. Experience has undeniably demonstrated that the strategic installation of adequate traffic safety facilities along roadways represents one of the most efficacious strategies for ensuring the safety of vehicular traffic. Nonetheless, the desert environment stands apart from the conventional roadside environment, presenting distinct challenges and considerations.The roadside vistas in deserts are characterized by vast emptiness, monotonous scenery, and a pervasive yellow backdrop. Prolonged driving on desert highways often leads to a diminished awareness of traffic safety facilities among drivers, fostering conditions conducive to fatigue driving and ultimately increasing the risk of traffic accidents.The phenomenon of driving fatigue has consistently garnered significant attention from researchers worldwide, underscoring its paramount importance and implications. In the context of navigating desert highways, the implementation of effective fatigue warning signs holds immense significance in alerting drivers and facilitating the study of fatigue characteristics, thereby enhancing overall road safety.

The origins of driver fatigue encompass both internal and external factors that contribute to the phenomenon.Chen GX, Natasha Merat, and their colleagues conducted an extensive examination of numerous traffic accident records, revealing that key factors such as age, driving experience, prolonged driving durations, and excessive speed significantly contribute to the onset of driving fatigue, ultimately leading to traffic accidents [2,3]. Upon analyzing traffic accident data, Laapotti et al. [4] discovered that male drivers exhibit a higher tendency to be involved in accidents stemming from fatigue, speeding, and other inappropriate driving behaviors compared to their female counterparts. Apart from the inherent reasons attributed to the driver themselves, external factors likewise play a pivotal role in precipitating fatigue-induced driving. Among these external factors, environmental monotony stands out as a significant contributor to fatigue-related driving. Farahman et al. [5] delved into the impact of monotonous road geometry on driver fatigue, uncovering that increased variations in road design correlate positively with improved driver performance and heightened vigilance. Chen Jianxin et al. [6]used a physiological feedback instrument to record the relevant physiological parameters of the driver, and selected theta waves in the brain waves to analyze the influence of external factors such as temperature, road conditions and sound on driving fatigue. Concurrently, a fatigue driving model can be formulated by assessing the driver's level of fatigue through the analysis of physiological parameters such as respiration rate, pulse, and electrodermal activity. This fatigue driving model has demonstrated a high degree of accuracy, exceeding 80 %, in predicting driver fatigue, as evidenced by studies conducted by Xie, Z. [7], Wang, Y.H. [8], and Wang, X [9].

Based on the causes of fatigue, there are subjective and objective methods for detecting driver fatigue characteristics. H Wang et al. [10] investigated the effects of driving fatigue on the reorganization of dynamic functional connectivity (FC) through newly developed temporal brain network analysis framework. C Chen et al [11] propose a self-attentive channel-connectivity capsule network for EEG-based driving fatigue detection to simultaneously reveal the intrinsic inter-channel relations that are known to be beneficial for EEG-based classification and reduce the high cost of data collection. H wang et al. [12] introduce a new attention-based multi-scale convolutional neural network-dynamical graph convolutional network model aiming to save time on parameter adjustment and thoroughly exploit the intrinsic inter-channel relations for classification. H wang et al. [13] extracted two types of features to explore the usefulness in driving experiment. T Xu et al [14] propose a unified framework to simultaneously perform personal identification and driving fatigue detection using a convolutional attention neural network. H wang et al. [15] proposed a fusion entropy analysis method of EEG and EOG. Guo Keyou [16] leveraged the Back Propagation neural network algorithm to develop a fatigue state detection system that relies on analyzing the driver's eye features. Tong Bingliang [17] devised a method to assess the driver's fatigue level by capturing and analyzing specific features of the driver's mouth. This approach informed the design and implementation of a driver fatigue state detection system. Shang Ting's research [18] revealed that eye signals serve as a reliable indicator of a driver's fatigue state. Specifically, the average rotation signal of the eyes can effectively reflect the driver's level of fatigue while operating a vehicle. Yeo et al. [19] analyzed and concluded that the beta wave of the EEG signal is more active when the driver is awake, and the alpha wave gradually becomes active as driving fatigue accumulates, and they established a support vector machine-based EEG fatigue discrimination method from this conclusion. Through monitoring surface electromyography (EMG) during grassland highway driving, Ma Aiying [20] observed that varying driving durations had differential impacts on the muscular fatigue of the driver's neck muscles. Notably, the most pronounced changes were observed between 35 and 70 min of driving, prompting the recommendation for drivers to take a break at the 70-min mark.

Charlton [21] aimed to rationalize road traffic signs by collecting empirical data on drivers' reactions to these signs while driving. The study analyzed the intricate interplay between the duration required for drivers to process traffic sign information and the temporal impact of this information across various driving scenarios. In a subsequent study, Charlton [22] investigated the variations in driver attention and comprehension when confronted with advance warning signs, contour markers, and road markings on flat curves.Koyuncu M et al. [23] delved into the response dynamics of driver groups when processing information presented through various traffic signs, taking into account their layout and the required driving speed. Their findings indicated that traffic information signs that integrate graphics and text produced the longest-lasting and most effective stimulus effect on drivers.

Upon conducting an exhaustive literature review, it becomes evident that there is a wealth of comprehensive research conducted internationally on the characteristics of driver fatigue. In China, the surge in the construction of desert highways has prompted a proliferation of studies on traffic safety within these unique environments, surpassing the volume of comparable research conducted abroad. Nonetheless, the current research landscape on driver fatigue characteristics and traffic sign placement in desert highway settings exhibits certain limitations. Domestically, most studies on traffic safety in desert highways focus on traffic accidents and highway design metrics, with a notable absence of research exploring driver behavior and responses to various traffic signs in the desert environment. While some research has ventured into investigating driver fatigue in desert conditions, the understanding of how roadside information can mitigate fatigue remains unclear and lacks specific, quantitative insights. Furthermore, the methodology for

installing traffic safety facilities that consider driver fatigue characteristics in desert environments is understudied. Consequently, conducting research on the deployment of fatigue warning signs on desert highways, leveraging cardiac and electromyographic indicators, holds significant value and potential to address these gaps. Meanwhile, in the literature exemplified above, many people use ECG and EMG for analysis, and it shows that these indicators and the development of fatigue all showed a normally distributed correlation, proving that physiological indicators are closely related to the fatigue changes. In this paper, we collect cardiac and electromyographic indicators to analyze the patterns of fatigue characteristics through field experiments as well as simulation experiments. At the same time, in order to ensure the authenticity and effectiveness of the simulation experiment, electrocardiogram data was selected to verify the simulation experiment. On this basis, several groups of simulation experiments with different fatigue warning signs and stimulation intervals were conducted. The data obtained after analyzing the change rule of cardiac and electromyographic indexes were processed by the artifact correction method, and the optimal fatigue warning signal setting method was obtained according to the processing results.

2. Methods

2.1. Experimental preparations

A comprehensive series of studies were executed on a dedicated test section of the Wuma Expressway, located within the Ningxia province of China, between the dates of September 20 and October 20, 2021.This particular segment of the highway was specifically closed off to public traffic, ensuring that the entire experimental process was conducted in a safe and controlled environment.The Ethics Committee of Chang'an University thoroughly reviewed and subsequently approved this experiment. Before the experiment commenced, all subjects were asked to fill in and sign an informed consent form. The designated experimental site received the official endorsement and approval from the Ningxia Transportation Design and Research Institute. All methodologies employed in the study were rigorously executed in strict adherence to the prevailing guidelines and regulations. The segment pertaining to electrocardiography is carried out in adherence to the Chinese standards and guidelines for dynamic electrocardiogram practice.Research endeavors that involved human participants were executed in conformity with the principles outlined in the Declaration of Helsinki. Confirm that the informed consent of all subjects has been obtained before the start of the experiment.

Simultaneously, the acquisition of ECG and EMG signals is straightforward, exhibiting minimal susceptibility to external influences and a relatively stable nature.The ECG signal acquisition process employs the HeaLink heart rate sensor, while the EMG Sensor dual-conductor module is utilized for capturing the EMG power curve. These equipment pieces boast robust anti-interference capabilities, a compact design for portability, and versatility in collecting data across diverse conditions. The driving simulation module, a six-degree-of-freedom platform crafted by FORUM8 in Japan, simulates road driving experiences. Moreover, supportive accessories like ECG film, pens, paper, and a laptop are also provided to facilitate the entire process.

Before the experiment, participants need to fill out a survey questionnaire.The driver's identifying information such as name, age, and work unit are counted. Considering the special characteristics of drivers driving in desert environments and the influence of personal experience on behavioral intention in the theory of planned behavior, drivers' experience of driving on desert highways should also be collected, and the main information collected can be categorized into whether they live there often, live there briefly, or drive on desert highways occasionally. The relevant content of the questionnaire is shown in Table 1 below.

2.2. Field fatigue driving experiment design

Internationally, it is common to limit driving time to reduce the hazards associated with fatigue driving, however, this method does not take the specific circumstances of different drivers, their mental state and the variability brought about by the road environment into account. During the driving process, human physiological indicators such as ECG and EMG are changed. Among them, heart rate variability and EMG power are good quantitative indicators for evaluating autonomic activity. Meanwhile, these two indicators are simple to collect and characterized by non-invasiveness and easy portability. In this experiment, ECG and EMG data were collected from drivers driving continuously on desert highways, and the heart rate variability, growth rate, and average EMG power were analyzed over time. The obtained data were compared and analyzed with the simulated driving data to verify the validity of the simulated driving experiment and the equivalent time relationship between simulated driving and actual driving.

2.2.1. Field experiment scene

It has been shown that drivers are most likely to feel fatigue from 11:00 to 17:00, so this time period was chosen as the experimental

Table 1
Relevant content of the survey questionnaire.

Name	Age
Driving experience (driving experience since obtaining a driver's license)	/years
Have you had any experience driving on desert highways:	No, occasional, frequent, year-round
Number of traffic accidents (cumulative):	0, 0–3, More than 3 times
How long do you think you will feel driving fatigue:	60–120 min, 120–180 min, over 180 min
The time period when driving is prone to fatigue	Time period

time. The experimental route is to drive into the highway from the toll station of the mixing station of Uma Expressway a9, drive to the main line direction of the a9 section from east to west, and then turn around from the a9 section to the end of the a10 section until driving to the junction of the a8 section and the a7 section, where there is no desert environment to stop. The actual alignment of the road is shown in Fig. 1.

2.2.2. Field experiment steps

Before driving into the experimental section, the participant put on the instruments and provide their personal information. During the experiment, the cardiac instrument was used to record the real-time heart rate changes of the participant, and the EMG instrument was used to record the EMG data of the neck muscles and the anterior bundle muscles of the shoulder. The locations of the heart rate electrode pads were the left lower chest and right upper chest. EMG was collected in two locations, with electrode pieces placed on both sides of the posterior erectile neck and on the right upper chest and anterior shoulder fasciculus, respectively. After the instrument started recording, the driver started driving, and the driving speed was controlled between 80 and 100 km/h according to the road design speed. The car was kept quiet to ensure a normal driving environment, and stopped recording after returning to the junction of section a8 and section a7. Then the driver will be asked to fill in the desert highway fatigue characteristics of factors affecting the structural equation modeling questionnaire, after observing the normal state of the subjects, the experiment is over, the next test subject will be invited to carry out the experiment. The scene of the experiment is shown in Fig. 2.

2.3. Simulation fatigue driving experiment design

2.3.1. Simulation experiment scene

To ensure the effectiveness of the simulated driving environment, based on the project design data and Baidu road network map, we conducted a field survey on the a8, a9 and a10 bid sections of Wuma Expressway in Tengger Desert, Zhongwei City, Ningxia Hui Autonomous Region, and carried out a three-dimensional visual scene simulation in uc win road to try to approach the real road environment and ensure that the basic road alignment, roadside environment, lane width, etc. are consistent with the actual environment.To align with practical engineering scenarios, the experimental road configuration adopts a combination of a lengthy straight line segment in the plane, coupled with a circular curve featuring a large radius. The vertical curve design endeavors to mimic the natural terrain as closely as feasible. Reduce the amount of filling and excavation, making virtual experiments comparable to on-site experiments and minimize other variables as much as possible. The actual road alignment, experimental simulation alignment, road simulation scenes are shown in Figs. 3 and 4.

2.3.2. Simulation experiment steps

The research project, conducted on a designated test road segment of the Wuma Expressway in Ningxia province, China, spanned from September 20 to October 20, 2021. This isolated stretch of highway was exclusively used for the study, ensuring the safety of all participants and the experiment's integrity. Prior to its initiation, the project underwent rigorous ethical review and was granted approval by the Ethics Committee of Chang'an University. As part of this process, all subjects were required to provide their informed consent by completing a consent form, attesting to their understanding of the study's purpose, procedures, and potential risks. Furthermore, the Ningxia Transportation Design and Research Institute granted authorization for the use of the experimental site, ensuring compliance with all necessary permissions and regulations. Throughout the research, strict adherence to relevant guidelines and regulations was maintained, with the electrocardiography component specifically adhering to the Chinese standards for dynamic
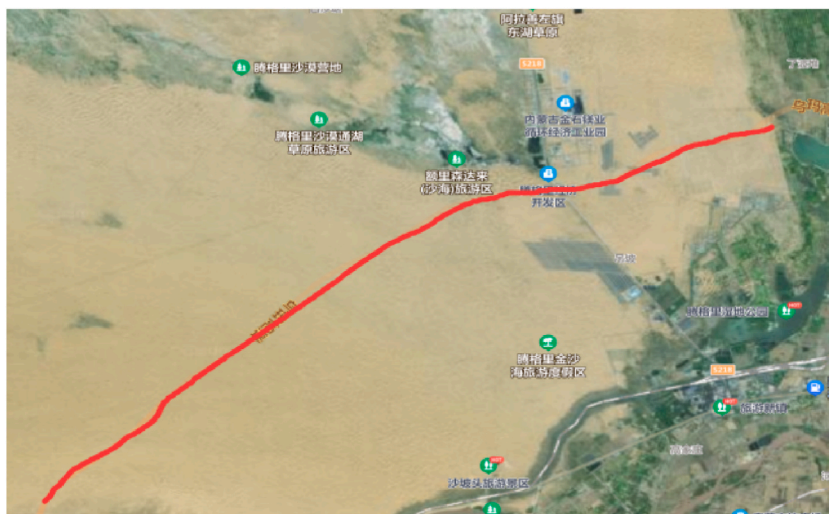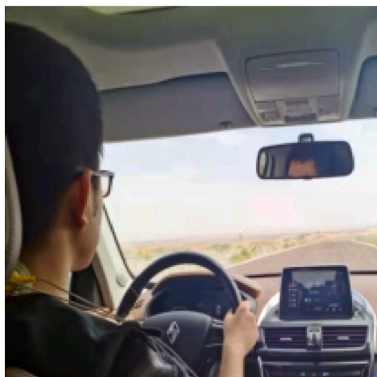

Fig. 1. Actual alignment of the highway.
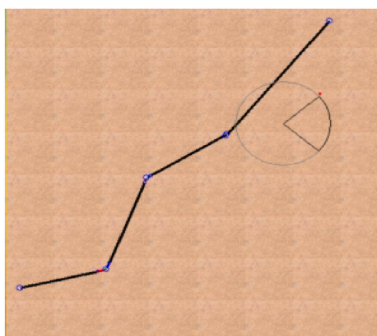
Fig. 2. Field experiment scene.

Fig. 3. Experimental simulated linear shape.

Fig. 4. Road simulation scenario.

electrocardiography. The study's human-centric approach aligns with the principles outlined in the Declaration of Helsinki, emphasizing ethical considerations in research involving human subjects. Importantly, it is confirmed that informed consent was obtained from every participant prior to their involvement in the experiment, safeguarding their rights and ensuring the study's ethical validity.

This paper analyzes the ECG and EMG signals of the subject drivers collected through driving simulation experiments to get their change rules over time to get the fatigue characteristics of the drivers in the driving process. The central electrical signal can respond to the driver's fatigue development state in the driving process, and the changes are more objective and realistic than other indicators. The EMG signal can respond to the driver's action and physiological changes in the driving process, interact with the ECG signal, and provide reference for the change law. At the same time, the ECG and EMG signals are easy to be acquired, less affected by the outside world, and relatively stable. The ECG signal acquisition equipment uses the HeaLink heart rate sensor and the EMG Sensor dual-conductor EMG sensor module to obtain the heart rate curve and EMG power curve respectively. The signal acquisition equipment has strong anti-interference ability, small size, easy to carry around, etc., and can be used for data acquisition under various states. The driving simulation module is a six-degree-of-freedom road driving simulation platform developed by FORUM8, Japan. In addition, there are other auxiliary equipment such as ECG film, pen, paper and laptop. The experimental scenario of the driving simulation

chamber is shown in Fig. 5.

A carefully selected cohort of 20 healthy drivers, aged between 20 and 50, each holding a valid driver's license and maintaining a regular work schedule, were recruited as participants for the study. Prior to the commencement of the experiment, cardiac electrodes were meticulously positioned, and real-time monitoring of heart rate and electromyography data from the steering wheel's control by the anterior shoulder beam was initiated. After thoroughly briefing the participants on the experimental protocols and precautions, the drivers embarked on their drive once the recording instruments were activated. An initial adaptation period of 5–10 min allowed the participants to settle into the driving process, during which time experimental real-time data was recorded. Throughout the drive, the speed was maintained within a range of 80–100 km/h, ensuring a safe and controlled environment. The laboratory was maintained in a state of quietude to mimic a normal driving environment, and this continued until the conclusion of the experiment upon reaching the end of the designated road segment. The driver's movements were observed throughout the experiment. During the observation process, the experimenter will observe the movements of the participants, such as the number of steering wheel rotations, neck rotations, and movements unrelated to driving, and record them.
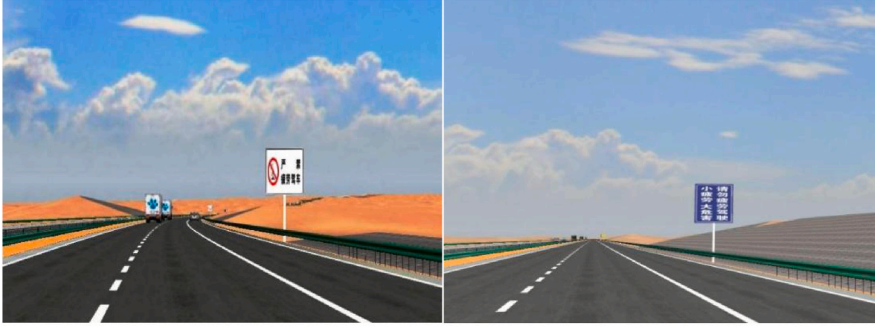
2.4. Traffic sign selection

According to the cardiac and electromyographic indexes obtained from the desert highway driving simulation experiment, the fatigue level generated by the driver at different times during the driving process was classified, and the fatigue characteristics and fatigue development law were obtained, the observational variables applicable to the indicator system of factors affecting driving fatigue were selected based on several internationally recognized fatigue survey scales. To address the varying degrees of driver fatigue encountered on desert highways, fatigue warning signs are strategically positioned with varying stimulation intervals and forms of stimulation. This tailored approach ensures that the signs are optimally effective based on the depth of fatigue experienced by drivers. By repeating the experimental process with different sets of signs, we aim to compare and analyze the stimulation effect of each group, ultimately identifying the optimal placement method for fatigue warning signs on desert highways. Drawing from previous experimental experience, it has been observed that the impact of traffic signs on electrocardiogram (ECG) readings is more pronounced during actual driving. Consequently, in this traffic sign stimulation experiment, we focus solely on analyzing the ECG index and its variation patterns. This targeted approach allows us to gain a deeper understanding of how the selected fatigue warning signs influence driver physiology, specifically their cardiac responses, under simulated desert highway driving conditions.

Highway Traffic Signs and Markings Specification (JTGD82-2009) [24], for driving safety reminder signs have the following provisions: square shape, black border, white lining; signs are generally black characters on a white background, black graphics, black border, graphic markings in the layout can be used in other colors if necessary. With regard to the setting position, it is stipulated that the setting of the notice sign shall not affect the setting and visual recognition of the warning, prohibition, instruction and wayfinding signs; and it is also added that the driving safety reminder signs such as the danger of drinking and driving, do not litter, fasten the seat belt, slow down at sharp curves and slow down at sharp curves and downslopes, etc. are added. The inner edge of the post sign shall not be less than 25 cm from the road surface (or shoulder), and the height of the lower edge of the signboard from the road surface shall be 180–250 cm. the inner edge of the post shall not be less than 25 cm from the road surface (or shoulder) 27.

Pursuant to the relevant regulations and guidelines, it is essential to investigate how traffic signs, particularly those designed to mitigate driver fatigue on desert highways, impact fatigue characteristics during prolonged driving. This analysis can be conducted by exploring two key aspects: the positioning of the fatigue warning signs and the color schemes employed in their design. To facilitate this study, several commonly used fatigue warning signs found on domestic highways have been selected and presented in Fig. 6(a–d). These signs represent a variety of design elements and placement strategies, providing a comprehensive basis for examining their effectiveness in combating driver fatigue under desert highway conditions.

Fig. 5. Experimental Scene of the cockpit simulation module.

(a) Red (black) characters on white background   (b) White letters on blue background

(c) Black text on white background   (d) Black letters on yellow background

Fig. 6. Four of four traffic signs selected for the simulation experiment.

3. Results

The results of the field experiment and the simulation experiment will be collected and processed. The data needs to be processed before it can be analyzed. The simulation experiments also need to be validated to prove that the simulation experiments are valid.

3.1. Data processing

The initially obtained ECG data are denoised based on an artifact correction algorithm. In the automatic artifact correction algorithm, artifacts are detected from the dRR sequence, which is a time series consisting of differences in successive RR intervals (the time between the appearance of two wave crests represents the end of a complete cardiac movement). dRR. sequences provide - a robust method to separate ectopic and misaligned heart beats from normal sinus rhythm. In this paper, a dynamic threshold (Th) is employed to distinguish between ectopic and physiological heartbeats. This threshold is calibrated based on the evolving distribution of the dRR (difference in adjacent RR intervals) sequence, facilitating adjustment to varying degrees of heart rate variability. For each heartbeat, the interquartile range deviation of the preceding and subsequent 90 beats is determined and scaled by a factor of 5.2. Ideally, if the RR series followed a normal distribution, this range would encompass 99.95 % of all beats. Nevertheless, given the non-normal nature of RR interval series, some normal beats may surpass this threshold. Consequently, the identification of robust algorithms becomes imperative for detecting spurious heart rates.Ectopic rhythms manifest in the dRR series through characteristic negative-positive-negative (NPN) or positive-negative-positive (PNP) patterns. Analogously, prolonged beats exhibit positive-negative (PN) patterns, while shortened beats display negative-positive (NP) patterns within the dRR series. Only segments of the dRR series that contain these patterns are classified as artifactual beats.Furthermore, the presence of missing or redundant heartbeats is detected by comparing the current RR interval value with the median of the 10 adjacent RR intervals (medRR). A missed beat is identified when the current RR interval (RR(i)) satisfies a specific criterion outlined in equation (1).

$$\left| \frac{RR(i)}{2} - medRR(i) \right| < 2Th \tag{1}$$

If two consecutive RR intervals (RR(i) and RR(i+1)) satisfy Eq. (2), an additional beat can be detected.

$$|RR(i) + RR(i+1) - medRR(i)| < 2Th \tag{2}$$

To refine the detection of ectopic beats, the corrupted RR time intervals are replaced with interpolated RR values, ensuring a smoother and more accurate representation of the heartbeat pattern. Similarly, anomalously long or short beats are corrected through interpolation of new RR time series values, aiming to normalize the heartbeat durations. Missing beats are addressed by inserting new R-wave onset times into the sequence, while extra, spurious beats are corrected by eliminating their R-wave detections and recal-culating the entire RR interval sequence accordingly.For the monitored data, the RR interval sequence was extracted using Kubios software, and subsequent corrections were performed by identifying noisy segments and applying an artifact correction algorithm. The effectiveness of these corrections is demonstrated in Fig. 7, showcasing improved accuracy and reliability in the heartbeat analysis.

3.2. Validation of validity of simulation experiments

The data collected in the field experiment were compared and analyzed with the data collected in the simulated driving experi-ment. Due to the certain differences in the habits and movements of different drivers when driving, and the different strengths of various movements will lead to large differences in EMG indicators, a poor fit will be caused when the simulated driving is subse-quently fitted with the actual driving. At the same time the heart rate of normal people fluctuates within a certain rangeand there is a certain trend with the increase of driving time, so the ECG data was selected to verify the validity of the driving simulation. Due to individual differences, the comparison analysis could not be done directly for the specific power values, but the base differences were denoised and processed for trend analysis. Observe whether the trend of both ECG indexes over time is consistent, and fit the two curves to a line, and verify the real validity of the simulated driving according to the fitting results. The heart rate growth rate index can better reflect the driver load and fatigue level, especially the driver's fatigue development state. Therefore, in this study, the heart rate growth rate is used to analyze the correspondence between simulated driving and actual driving. After the driver heart rate fitting curve is obtained, a calculation queue is selected in Kubios to obtain the heart rate growth rate of simulated driving and actual driving respectively. The obtained data were varied with the instrument recording points to obtain the heart rate growth rate curve as shown in Figs. 8 and 9, where the horizontal coordinates are the points recorded over time during instrument acquisition and the vertical co-ordinates are the heart rate growth rate.

According to the analysis of the heart rate growth rate curves during the simulation and actual driving, both of them showed a fluctuating change of falling, then rising and then falling, and the overall direction change was the same. This is in line with the existing recognized development process of driving fatigue [25] , i.e. initial fatigue, adjustment and fatigue deepening. The time correspon-dence between simulated driving and actual driving in the three stages of change based on heart rate growth rate showed an obvious linear relationship, and the fitting results were high, $R2 = 0.95$, which proved that the simulated experiment and the actual experiment were consistent with each other. The time correspondence between the two was expressed as a segmental function as shown in Equation (3), where y is the actual driving time (min) and x is the simulated driving time (min).

$$\begin{cases} y= 4.34074 + 2.4512x \\ y= 53.40976 + 2.06788x \\ y= -259.16892 + 3.55921x \end{cases} \tag{3}$$

From the line fitting results of the two, it can be seen that the simulated driving system can truly and effectively reflect the actual driving process. At the same time, there is a correspondence between the simulated driving time and the actual driving time. 60 min of simulated driving on the desert highway corresponds to 120–180 min of driving time in the actual desert highway. In the subsequent analysis of the change curve of each index with time, the analysis can be carried out according to the actual driving time corresponding to the simulated driving time to improve the analysis efficiency.
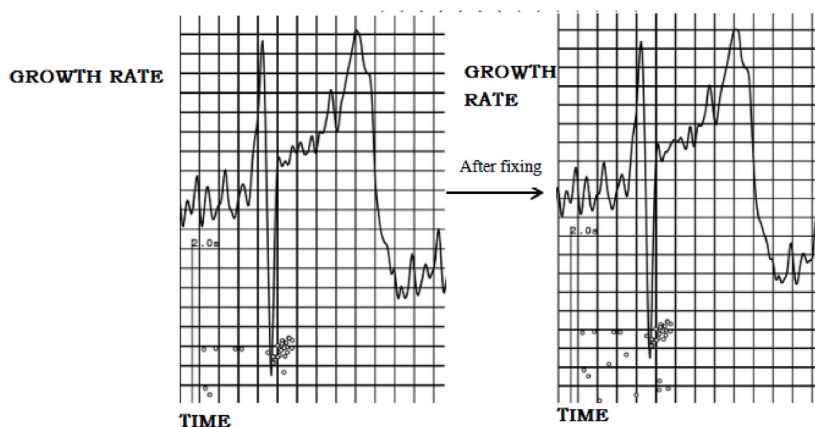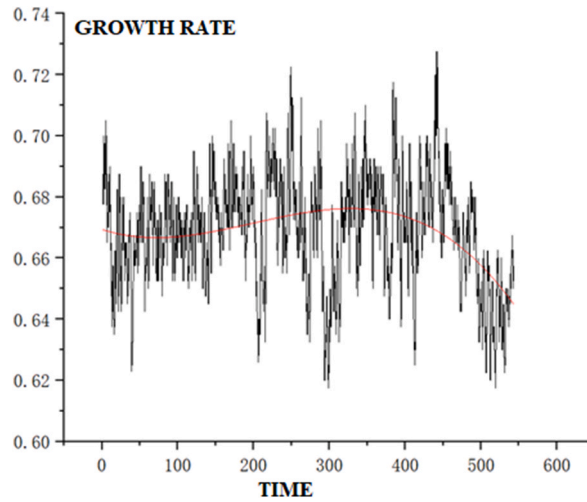

Fig. 7. ECG signal correction result.

Fig. 8. Simulated experimental heart rate growth rate curve.
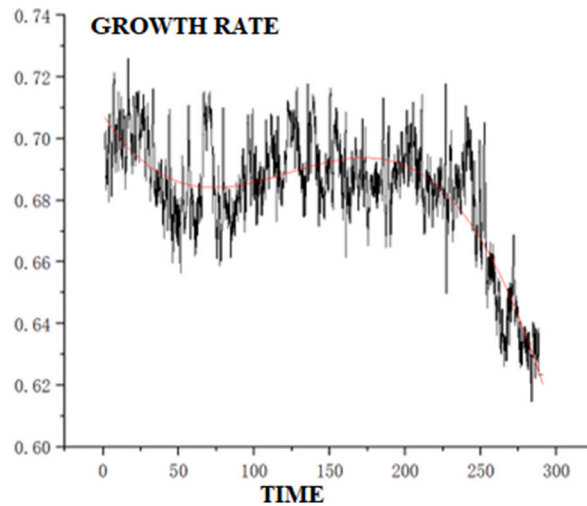

Fig. 9. Actual experimental heart rate growth rate curve.

4. Discussion

4.1. Analysis of cardiac and myocardial electrical patterns

Based on the cardiac and myoelectric data collected in the driving simulation experiment, the standard deviation of sinus RR interval (SDNN) and myoelectric power in the heart rate variability index were selected as the indexes for analyzing the degree of driver fatigue.

The standard deviation of normal sinus RR interval (SDNN) is calculated by Equation (4).

$$SDNN = \sqrt{\frac{\sum\limits_{i=1}^{N}(RR_i - meanRR)^2}{N}} \tag{4}$$

The term RR_i represents the i-th heartbeat interval, whereas mean RR signifies the average of N such intervals. SDNN, serving as a metric, quantifies the overall extent of variability in heart rate (HRV). Specifically, an SDNN value below 100 ms indicates a moderate reduction in HRV, while an SDNN lower than 50 ms denotes a significant decrease. Consequently, if SDNN is less than 50 ms, HRV is classified as low; conversely, an SDNN equal to or greater than 100 ms signifies high HRV. The SDNN variation curve over time is shown in Fig. 10.

The analysis presented in Fig. 10 reveals that throughout the simulated driving session, the SDNN index ranged between 50 and
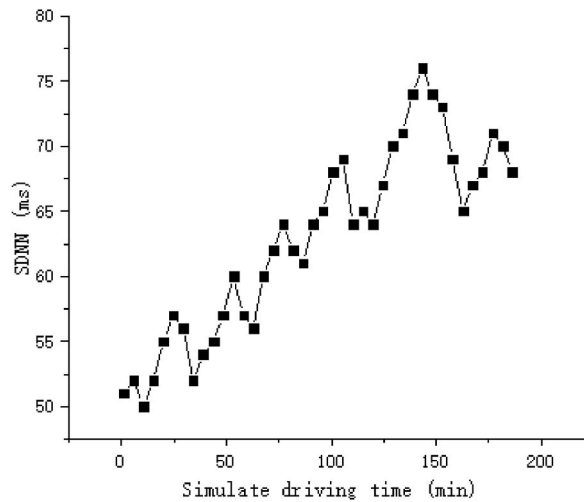
Fig. 10. SDNN change curve over time.

100 ms, suggesting a gradual decline in the driver's HRV activity as driving duration progressed. Notably, the mean heart rate steadily decreased, accompanied by an elongation of the R–R intervals. The SDNN, a time-domain metric primarily indicative of sympathetic nervous system activity, exhibited a notable overall increase, which correlated significantly with an intensification of fatigue levels during the driving process.During the initial 30 min of driving, the indicator experienced mild fluctuations. Subsequently, from 30 to 70 min, a distinct upward trend in fluctuations was evident. Approaching 150 min, the indicator gradually declined, followed by a period of gentle oscillation and a slight upward trend lasting until roughly 170 min. Afterward, it gradually increased and eventually stabilized, demonstrating a clear phased fluctuation pattern throughout the entire driving duration. The change curve of SDNN over time can show that the gentle fluctuation at the beginning of about 30 min is mainly due to the fact that the drivers have had sufficient adaptive training on the driving simulator before the formal test, and they can adapt to the simulated driving environment very well, and the overall mind of the drivers is more relaxed, with gentle fluctuation of SDNN, constant HRV activity, and a smoother heart rate. Due to the monotonous and less stimulating environment on the roadside of the desert highway [26] , the psychological state of the drivers changed, and most of the drivers would experience some boredom and irritability after 30 min. The driver's psychological state underwent alterations, with the majority experiencing boredom and irritability after approximately 30 min of driving. This was mirrored in the steep linear increase of SDNN, a reduction in HRV activity, and a deepening of fatigue levels. Recognizing their exhaustion, drivers would actively seek to adjust, resulting in noticeable fluctuations of the SDNN index around the 80-min mark. However, by approximately 120 min, the driver's capacity for proactive adjustment diminished, and fatigue progressively intensified. Reaching a peak around 150 min, HRV activity continued to decline, signifying a significant aggravation of fatigue. Despite further attempts at adjustment, the driver remained in a state of persistent fatigue thereafter. The core mechanism of muscle fatigue involves the sustained depletion of muscle glycogen stores until exhaustion. This process is directly mirrored by alterations in power output, which serves as a tangible indicator of energy dynamics. Table 2 presents the power values recorded during EMG acquisition at specific intervals throughout the experiment, while Fig. 11 illustrates the temporal variation of the average power derived from surface EMG measurements.11.

According to the analysis in Fig. 11, the overall logarithmic value of the average power of the EMG signal shows a fluctuating

Table 2
The EMG acquisition power values during a certain period.

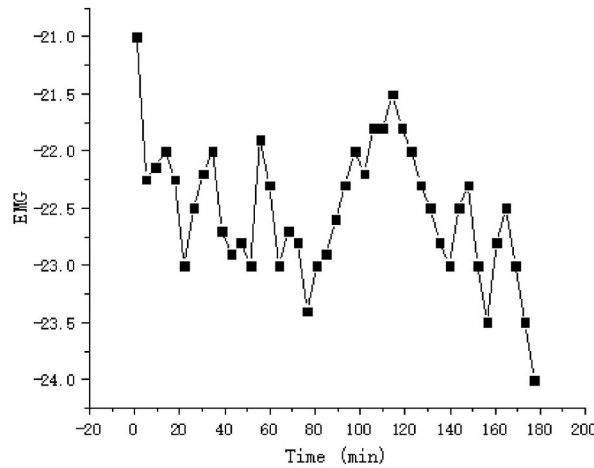| Time(s)	Average value	Collection value	Power value	Muscle strength
5	1509	1506	16	0
6	1509	1511	7	0
7	1509	1506	6	0
8	1509	1513	5	0
9	1509	1498	5	0
10	1509	1498	5	0
11	1509	1490	6	0
12	1509	1490	6	0
13	1510	1490	6	0
14	1510	1509	7	0
15	1510	1509	7	0
16	1510	1527	24	0
17	1511	1527	24	0
18	1510	1527	24	0

Fig. 11. Plot of the mean power change of EMG signal over time.

decrease (average decrease V = 0.26 times/min) in the early stage, an obvious linear increase in the middle and late stages, and a fluctuating decrease in the late stages that eventually plateaus. The experimental accuracy measured by the instrument is adjustable, because the measured muscle substantial changes are small, so the data of substantial changes in muscle power are not recorded, so they are all 0. The overall basic presentation unfolded in four distinct phases. Within the first 40 min of driving, the average EMG power underwent significant fluctuations without a discernible upward or downward trend, reflecting the driver's heightened alertness and increased activity such as adjusting the driving route and turning the steering wheel more frequently. Between 40 and 80 min, the average EMG power gradually declined, signifying the onset of fatigue and a reduction in the driver's movements. From 80 to 140 min, the average EMG power gradually increased and peaked, indicating that the driver was actively engaging in frequent actions to combat fatigue. Beyond 140 min until the end of the experiment, the average EMG power fluctuated but generally continued to decrease, suggesting a gradual decline in the driver's ability to adjust and a deepening of fatigue levels.

4.2. Interaction analysis of cardiac and myoelectric indices

Given that both indicators share the same frequency unit, they were quantitatively assessed and analyzed to uncover the fatigue characteristics arising from the interplay between cardiac and myoelectric activity during the desert highway simulation experiment. The temporal variations of these cardiac and electromyographic indices are visually represented in Fig. 12.

An analysis of Fig. 12 reveals that both ECG and EMG signals of the driver during the simulated driving exhibited pronounced fluctuations that intensified with the progression of driving time. These changes discernibly unfolded in four distinct stages: (1) an initial fluctuation phase for cardiac (0–25min) and myoelectric (0–35min) indices; (2) a continuous rise phase for cardiac (25–75min) and myoelectric (35–85min) indices; (3) a fluctuating rise phase for ECG (75–170min) and EMG (85–140min); and (4) a steady phase for ECG (170–200min) and EMG (140–200min). Statistical descriptions of the magnitudes of ECG and EMG variations, along with the sizes of fluctuations within each time period, are presented in Table 3.
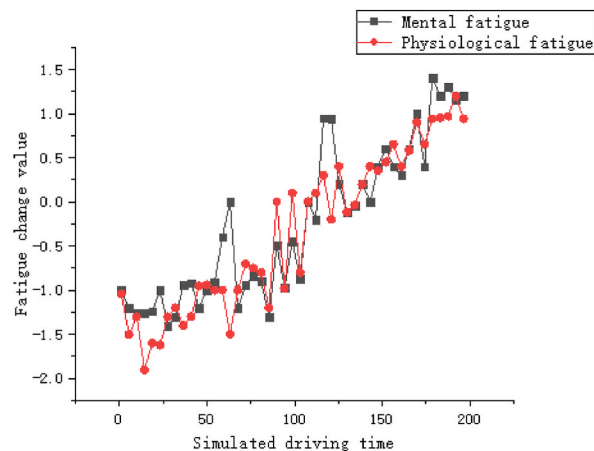

Fig. 12. Curves of cardiac and EMG indicators over time.

Table 3
Change statistics of ECG and EMG indicators.

	N Statistical quantity	Full distance Statistical quantities	Minimal value Statistics	Maximum value Statistics	Mean value Statistics	Mean Value Standard Error	Standard deviation Statistical quantity	Variance Statistical volume
ECG(1)	7	0.360	−1.370	−1.010	−1.132	0.043	0.113	0.013
EMG (1)	9	0.620	−1.570	−1.130	−1.375	0.061	0.184	0.034
ECG(2)	9	1.300	−1.140	0.150	−0.599	0.136	0.408	0.167
EMG (2)	9	0.770	−1.310	−0.530	−0.851	0.076	0.229	0.053
ECG(3)	20	1.870	−1.230	0.650	−0.246	0.100	0.407	0.187
EMG (3)	12	2.110	−1.090	1.020	−0.019	0.190	0.598	0.304
ECG(4)	15	2.570	−0.100	2.40	1.157	0.215	0.831	0.691
EMG (4)	21	1.420	0.060	1.480	0.899	0.088	0.403	0.162

Based on the statistics in Table 3 and it can be concluded that, during the first stage, the ECG index experienced brief fluctuations with minimal variation in both indices, as evidenced by low standard deviation and variance values. This suggested that the driver's fatigue state remained relatively unchanged, indicating they had not yet entered a state of fatigue. In contrast, during the second stage, both indices displayed an upward trend, with the ECG index exhibiting a 1.69 times greater increase compared to the EMG index, as revealed by the full distance statistics. At the same time, the standard deviation and variance values of the two indicators are larger, which proves that the fluctuation of the two indicators is larger, indicating that the phenomenon of driving fatigue begins to appear during the driving process in this period, and the psychological fatigue represented by the ECG indicators appears earlier than the physiological fatigue represented by the EMG indicators. In the third stage, the driver's fatigue continued to deepen, but both indicators showed certain fluctuations, representing that the driver gradually began to adjust and try to alleviate the deepening of fatigue during the driving process. The variance 0.304 and standard deviation 0.598 of EMG indicators were greater than the variance 0.187 and standard deviation 0.407 of ECG indicators, which shows that the fluctuation of EMG indicators was greater than that of ECG indicators, indicating that the effect of physiological adjustment of drivers is more obvious than that of psychological effect. However, physiological fatigue is also deeper than psychological fatigue. In the last stage, the ECG and EMG indicators did not show obvious fluctuations, and both indicators steadily increased and gradually stabilized, and the full distance statistic of ECG indicators reached a peak of 2.570, indicating that the deepening of psychological fatigue was more obvious at this time, and the driver's adjustment effect was insufficient at this time and entered deep fatigue.

Based on the aforementioned analysis, it is evident that during the desert highway simulation driving, the driver begins to experience both mental and physiological fatigue after approximately 35 min of driving. As the driving time extends beyond 85 min, the fatigue level gradually intensifies, prompting the driver to initiate adjustments. Notably, these adjustments effectively mitigate physiological fatigue. However, after 140 min of driving, the fatigue level escalates further, with the driver's ability to adjust diminishing, ultimately leading to a state of profound fatigue that significantly jeopardizes driving safety.

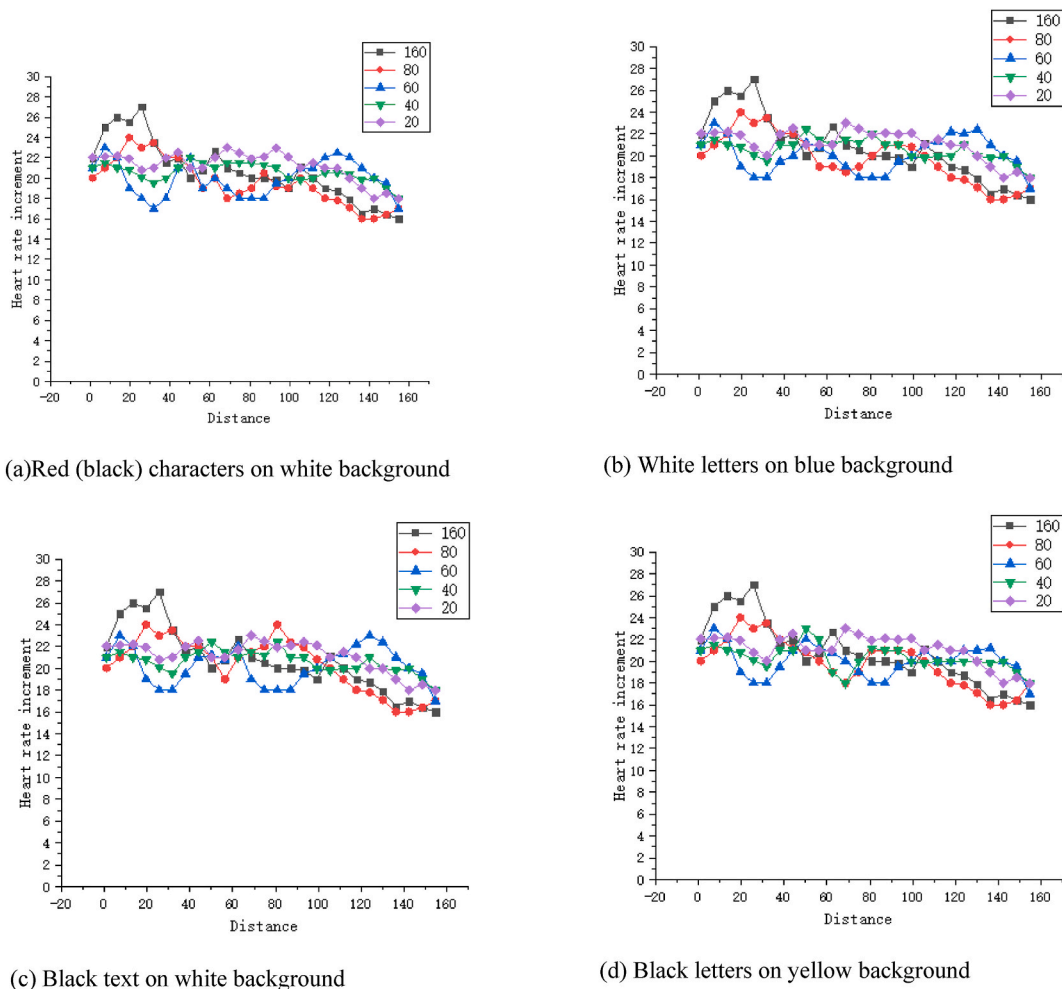
(a)Red (black) characters on white background

(b) White letters on blue background

(c) Black text on white background

(d) Black letters on yellow background

Fig. 13. Curve of traffic sign heart rate increment over time in the four groups.

4.3. Analysis of the pattern of electrocardiographic indicators under the stimulation of traffic signs

The four commonly used fatigue warning signs in section 2.3 were selected, namely (a) red (black) letters on a white background, (b) white letters on a blue background, (c) black letters on a white background, and (d) black letters on a yellow background, hereinafter referred to as (a) (b) (c) (d) four traffic signs. Psychological researchers (Kang Qiuyi, Tao Jin&Zheng Yang, 2010) have shown that too much stimulation within a certain period of time will significantly weaken the effect of such stimulation, so there should be a reasonable range of stimulation setting interval. According to the fatigue development time corresponding to the above analysis results and the design speed of 80 km/h, the corresponding stimulation setting distance range is 0–160 km. The five experimental scenarios were designed according to the stimulus setting interval, which were 80 km, 60 km, 40 km, 20 km and 160 km, among which 160 km was no stimulus setting. The experimental procedure is consistent with the above fatigue characteristics experiments, and only ECG data were extracted from the experimental results because ECG data are more obvious in response to the stimulation effect. The ECG index was selected as the heart rate increment, which is defined as due to the existence of individual driver variability. In order to more realistically and accurately characterize the changes in the heart rate of the subject, the heart rate increment at a certain moment in time can generally be chosen as the indicator for evaluation. The calculation 5 is shown below.

$$d\_n(t0) = N(t0) - \overline{n} \ (t0 = 1; 2; 3) \tag{5}$$

d_n(t0) - the increment of heart rate at a moment in bpm.
N(t0)-the actual heart rate value at a moment in bpm.
$\overline{n}$ - the average heart rate value of the driver at rest in bpm.

The heart rate increment curves over time for the five stimulus scenarios under four sets of traffic signs are shown in Fig. 13(a-d).

According to previous studies [27], Chen Xuanru&Shi Lemin, 2020), as the driver's psychological stress level intensifies, the magnitude of heart rate increment escalates. Fig. 13 depicts a consistent trend of diminishing heart rate increment across all four traffic sign stimuli as driving time or distance accumulates. In examining the relationship between heart rate increment and stimulation points, the influence of traffic sign placement and color scheme on heart rate was taken into account. Analyzing the heart rate increment timelines for the four groups of traffic signs, it becomes evident that their variation patterns are fundamentally similar. Consequently, the average rates of change for each curve under the five stimulus conditions were extracted and presented in Table 4.

Accoding to the analysis in Tables 4 and it can be seen that the trend of drivers' changes during driving on the desert highway under the stimuli of different traffic sign setting distances is consistent, and all of them will produce certain heart rate changes. Under the four stimuli, the incremental stimulation of heart rate is most obvious when the traffic signs are set at 60 km intervals, the incremental stimulation of heart rate at 80 km intervals and 40 km intervals are basically equivalent, and the incremental stimulation of heart rate is lower when the intervals are set at 20 km intervals. Therefore, considering the cost of setting traffic signs and the mutual influence with other traffic signs, it is unreasonable to set fatigue warning signs at 20 km intervals. Among the four kinds of traffic signs, the effect of setting black letters on white background stimulates the most obvious, and the rate of change is the highest among the four kinds of traffic signs, all of which are more than 19 %. Through the analysis of driving simulation, it can be obtained that the traffic signs with black characters on white background are set at an interval of 60–80 km to stimulate driving fatigue on the desert highway most obviously.

4.4. Determination of fatigue level based on cohesive hierarchical system clustering analysis method

To validate the appropriateness of fatigue warning sign placement, it is crucial to select cardiophysiological fatigue-specific indicators for cluster analysis, enabling the stratification of fatigue levels and thus facilitating timely reminders tailored to varying degrees of fatigue. This study employs a cohesive hierarchical clustering approach to categorize fatigue states. Drawing from prior research, a complete fatigue cycle, progressing from initial to severe fatigue, can manifest within 4 h of simulated driving, encompassing four distinct stages: awake, mild fatigue, moderate fatigue, and severe fatigue. Consequently, this paper designates four clusters to correspond with these stages. Within the systematic clustering framework, each fatigue indicator and indicator group undergoes separate clustering. Given the similarity in clustering procedures, this paper exemplifies the clustering process using the cardiac index SDNN, with details and outcomes presented in Table 5.

Table 5 illustrates the dynamic variations of SDNN indicators over a 4-h simulated driving period, categorized into four clusters reflecting the successive stages of fatigue emergence, progression, adjustment, and deepening. The table reveals that the first cluster corresponds to the awake state lasting from 0 to 30 min, followed by mild fatigue from 35 to 85 min, moderate fatigue and adjustment spanning 85–160 min, and finally, severe fatigue beginning at 165 min. The clustering fluctuations observed in the table signify substantial adjustments made by the driver during these designated time intervals, resulting in notable fluctuations in the indicator values, which may even drop into the range characteristic of the preceding fatigue stage. Such phenomena give rise to the outcomes presented in the table. Utilizing the outcomes of the aforementioned clustering, specifically the temporal segmentation of fatigue stages, the mean and standard deviation of SDNN indices within each time segment were determined as the SDNN fatigue thresholds for that particular period. This same processing methodology was applied to each fatigue index, encompassing SDNN and other relevant indicators. A summary of the cluster analysis pertaining to the comprehensive fatigue indicators is presented in Table 6.

The following conclusions can be obtained from the analysis presented in Table 6. In the desert highway simulation driving process, within 35 min, the driver exhibits comprehensive fatigue symptoms, signifying the concurrent onset of both psychological and physiological fatigue. After 110 min, the fatigue level intensifies, where both psychological and physiological fatigue deepen, resulting

Table 4
The change rate of each stimulus point of the four traffic signs.

	80	60	40	20
(1)	19.0 %	19.6 %	18.7 %	17.0 %
(2)	17.6 %	19.4 %	19.0 %	17.4 %
(3)	19.5 %	20.4 %	19.4 %	17.6 %
(4)	18.0 %	19.2 %	19.0 %	17.4 %

Table 5
SDNN metric clusters.

Time(min)	4 Cluster	3 Cluster	2 Cluster	Time(min)	4 Cluster	3 Cluster	2 Cluster
5	1	1	1	105	3	2	2
10	1	1	1	110	3	2	2
15	1	1	1	115	3	2	2
20	1	1	1	125	3	2	2
25	1	1	1	130	3	2	2
30	1	1	1	135	3	2	2
35	2	1	1	140	3	2	2
40	2	1	1	145	3	2	2
45	1	1	1	150	3	2	2
50	2	1	1	155	3	2	2
55	2	1	1	160	3	2	2
60	2	1	1	165	3	2	2
65	2	1	1	170	3	2	2
70	2	1	1	175	4	3	2
80	3	2	2	180	4	3	2
85	3	2	2	185	4	3	2
90	3	2	2	190	4	3	2
95	3	2	2	195	4	3	2
100	3	2	2	200	4	3	2

Table 6
Summary of cluster analysis of comprehensive fatigue indicators.

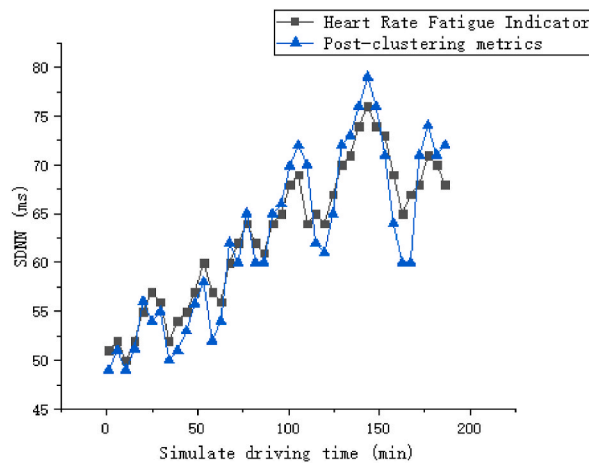| Fatigue level	Sobriety Time Period (min)	Mild fatigue Time Period (min)	Fatigue development Time period (min)	Severe fatigue Time Period (min)
Mental fatigue	0–30	35–155	155–180	180–200
Physiological fatigue	0–45	50–110	115–160	160–200
Comprehensive fatigue	0–35	40–110	115–160	170–200

Fig. 14. Comparison of heart rate fatigue index and post-clustering index.

in a corresponding increase in the overall fatigue degree. Beyond 160 min, the fatigue continues to deepen further, progressing into the severe fatigue stage. At this time, due to psychological fatigue, physiological fatigue are in a deeper fatigue stage, the joint effect leads to the early arrival of severe comprehensive fatigue time period. Based on the driving fatigue threshold identified for the desert highway, the optimal location for installing fatigue warning signs is during the period when drivers begin to experience mild fatigue on the highway, prior to the onset of severe fatigue. For the desert highway section designed with a speed limit of 80 km/h, the traffic sign setting intervals corresponding to the fatigue level were compared with the traffic sign spacing distances determined after the psychological fatigue experiment, and the results are shown in Fig. 11.

A comparative analysis of the SDNN indices depicted in Fig. 14 reveals that the two plotted curves align closely, exhibiting a gradual and smooth upward trend from 0 to 100 min. During the initial 0–70 min, the rate of change in SDNN indices post-clustering slightly surpasses that of heart rate SDNN indices, with the most notable difference in the rate of change occurring around 50 min, albeit maintaining a similar overall trend. Between 100 and 150 min, the SDNN index value continues to increase gradually, with the maximum post-clustering SDNN index exceeding the heart rate fatigue index by just 5 ms. In the subsequent 150–200 min period, both indices display a gradual downward trend, wherein the minimum post-clustering SDNN index is 6 ms higher than the heart rate fatigue index. Considering the maximum and minimum values, rates of change, and overall trends, it can be inferred that the fatigue progression pattern as determined by the heart rate fatigue SDNN index closely aligns with the fatigue levels derived from the clustering analysis, thereby reinforcing the validity of the fatigue threshold classification results. Through a comparative analysis of fatigue thresholds and heart rate fatigue indices, calculated based on driving speeds ranging from 80 to 100 km/h, it can be validated that positioning fatigue warning signs at intervals of 60–80 km represents a reasonable strategy.

5. Conclusion

By replicating the actual desert highway scenario in a driving simulation experiment, cardiac and myoelectric data were gathered from participating drivers. By selecting pertinent cardiac and myoelectric indicators, a change curve was plotted against driving time, followed by statistical analysis of the data. This comprehensive approach led to the following key conclusions.

(1) The simulated driving system can truly and effectively reflect the actual driving process. At the same time, there is a corresponding relationship between the simulated driving time and the actual driving time. The simulated driving of 60min desert highway corresponds to the driving time of 120–180min in the actual desert highway.

(2) Utilizing an artifact correction method to purify ECG data, an analysis of the measured data reveals that during desert highway driving, psychological fatigue precedes physiological fatigue as driving duration increases. Specifically, mental fatigue onset is observed at approximately 30 min of driving, with a more pronounced adjustment effect occurring around 80 min. Fatigue intensity gradually escalates past 120 min, peaking at 150 min before fluctuating in a stabilized manner. Conversely, physiological fatigue initially manifests at 40 min of driving, with a notable adjustment period spanning 80–140 min, followed by a continual deepening of fatigue thereafter.

(3) An examination of the interplay between cardiac and electromyographic indices reveals that during the initial 35 min of desert highway driving, both indices remain relatively stable, indicating no significant fatigue. However, within 85 min, both indices fluctuate and elevate, signifying the emergence of preliminary fatigue. At 140 min, cardiac indices exhibit a slightly more pronounced increase than electromyographic indices, prompting the driver to actively counteract fatigue, with a more visible adjustment effect observed for physiological fatigue. Beyond 140 min, fatigue intensity intensifies, and the driver's ability to mitigate fatigue gradually diminishes, ultimately progressing into a state of profound fatigue.

(4) Through the ECG data collected from driving simulation experiments with different stimulation intervals of four kinds of traffic signs in multiple groups, the heart rate increment curve with time was established for each group. Comparative analysis shows that for the desert highway, the fatigue warning sign with black letters on a white background set at intervals of 60–80 km is the most obvious stimulus for driving fatigue on the desert highway compared with the other three traffic signs.

(5) Utilizing the cohesive hierarchical system clustering analysis approach for classifying fatigue levels, a comparative analysis of fatigue thresholds and heart rate fatigue indices, tailored to driving speeds ranging from 80 to 100 km/h, validates that installing fatigue warning signs at intervals of 60–80 km is a practical and reasonable strategy. This study exclusively constructed a driving simulation environment that mirrored the real-world scenario, focusing solely on three cardiac and myoelectric metrics: SDNN, heart rate increment, and average myoelectric power. Additionally, while the potential for conducting actual desert highway driving experiments and analyzing a broader spectrum of cardiac and myoelectric indices against simulation data was acknowledged, such endeavors are slated for further exploration in subsequent research endeavors.

Funding

Data availability statement

The data used to support the findings of this study are included within the article.
Sharing research data helps other researchers evaluate your findings, build on your work and to increase trust in your article. We

encourage all our authors to make as much of their data publicly available as reasonably possible. Please note that your response to the following questions regarding the public data availability and the reasons for potentially not making data available will be available alongside your article upon publication.

Has data associated with your study been deposited into a publicly available repository? No.

Please select why. Please note that this statement will be available alongside your article upon publication.as follow-up to "Data Availability.

" Sharing research data helps other researchers evaluate your findings, build on your work and to increase trust in your article. We encourage all our authors to make as much of their data publicly available as reasonably possible. Please note that your response to the following questions regarding the public data availability and the reasons for potentially not making data available will be available alongside your article upon publication.

Has data associated with your study been deposited into a publicly available repository? Data included in article/supp. material/ referenced in article.

CRediT authorship contribution statement

Xingang Wang: Visualization, Supervision. **Xiangyun Hu:** Writing – review & editing, Writing – original draft, Investigation, Conceptualization. **Xingli Jia:** Resources. **Zexuan Jiao:** Methodology, Data curation.

Declaration of competing interest

The authors declare that the research was conducted in the absence of any commercial or financial relationships that could be construed as a potential conflict of interest.

Appendix A. Supplementary data

Supplementary data to this article can be found online at https://doi.org/10.1016/j.heliyon.2024.e36431.

References

[1] Q.L. Liu, Y.B. Zhang, B. Zou, Characteristic analysis and countermeasures of road traffic accidents in China, Chinese Journal of Safety Science 6 (2006) 123–128 + 145.
[2] G.X. Chen, et al., NIOSH national survey of long-haul truck drivers: injury and safety, Accid. Anal. Prev. 85 (DEC) (2015) 66–72.
[3] N. Merat, A.H. Jamson, The effect of three low-cost engineering treatments on driver fatigue: a driving simulator study, Accid. Anal. Prev. 50C (1) (2013) 8–15.
[4] S. Laapotti, E. Keskinen, Has the difference in accident patterns between male and female drivers changed between 1984 and 2000? Accid. Anal. Prev. 36 (4) (2004) 577–584.
[5] B. Farahmand, A.M. Boroujerdian, Effect of road geometry on driver fatigue in monotonous environments: a simulator study, Transport. Res. F Traffic Psychol. Behav. 58 (OCT) (2018) 640–651.
[6] J.X. Chen, X. Cheng, F. Chen, Analysis of the influencing factors of highway driving fatigue, Highway Traffic Science and Technology (Applied Technology Edition) 6 (6) (2010) 265–268.
[7] Z. Xie, Research on Driving Fatigue Model Based on Physiological Signals [D], Soochow University, 2017.
[8] Y.H. Wang. Short-term recovery characteristics of driving fatigue under simple landscape environment on grassland roads 137, Inner Mongolia Agricultural University, 2019, pp. 10–122.
[9] X. Wang, Research on the Influence of Long Straight Line in Desert Grassland on Driver's Vision and Heart rate[D], Ningxia University, 2018.
[10] H. Wang, X. Liu, H. Hu, F. Wan, T.P. Jung, Dynamic reorganization of functional connectivity unmasks fatigue related performance declines in simulated driving, IEEE Trans. Neural Syst. Rehabil. Eng. (99) (2020).
[11] C. Chen, Z. Ji, Y. Sun, A. Bezerianos, N.V. Thakor, H. Wang, Self-attentive channel-connectivity capsule network for eeg-based driving fatigue detection. IEEE Transactions on Neural Systems and Rehabilitation Engineering, a publication of the IEEE Engineering in Medicine and Biology Society, 2023.
[12] H. Wang, L. Xu, A. Bezerianos, C. Chen, Z. Zhang, Linking attention-based multi-scale cnn with dynamical gcn for driving fatigue detection, IEEE Trans. Instrum. Meas. 57 (3) (2020), 1-1.
[13] Wang, H. , Liu, X. , Li, J. , Xu, T. , Bezerianos, A. , & Sun, Y. , et al. Driving fatigue recognition with functional connectivity based on phase synchronization. IEEE Transactions on Cognitive and Developmental Systems, PP(99), 1-1.
[14] Xu, T. , Wang, H. , Lu, G. , Wan, F. , & Sun, Y. . (2021). E-key: an eeg-based biometric authentication and driving fatigue detection system. IEEE Transactions on Affective Computing, PP(99).
[15] Wang, H. , Wu, C. , Li, T. , He, Y. , & Bezerianos, A. . (2019). Driving fatigue classification based on fusion entropy analysis combining eog and eeg. IEEE Access, PP(99), 1-1.
[16] K.Y. Guo, C.Y. Zhang, Vision-based driver fatigue and attention monitoring method, Highway Traffic Technology 27 (5) (2010) 104–109.
[17] B. Tong, Monitoring of Fatigue Driving and Mental Dispersion Monitoring Based on Mouth State [D], Jilin University, 2004.
[18] T. Shang, Research on Key Parameters of Road Visual Speed Control Marking Based on Driver's Eye Movement characteristics[D], Chongqing Jiaotong University, 2017.
[19] M. Yeo, Li X, K. Shen, et al., Can SVM be used for automatic EEG detection of drowsiness during car driving? Saf. Sci. 47 (1) (2009) 115–124.
[20] A.Y. Ma, Research on the Neck Muscle Fatigue Model of Grassland Highway Drivers Based on Surface Electromyography [D], Inner Mongolia Agricultural University, 2017.
[21] S.G. Charlton, Conspicuity, memorability, comprehension, and priming in road hazard warning signs, Accid. Anal. Prev. 38 (3) (2006) 496–506.
[22] S.G. Charlton, The role of attention in horizontal curves: a comparison of advance warning, delineation, and road marking treatments, Accid. Anal. Prev. 39 (5) (2007) 873–885.
[23] M. Koyuncu, S. Amado, Effects of stimulus type, duration and location on priming of road signs: implications for driving, Transport. Res. F Traffic Psychol. Behav. 11 (2) (2008) 108–125.
[24] JTGD82-2009, China Highway Traffic Signs and Markings Specifications[S].

[25] Zhenwei Duan, Jing Guoxun, Yang Shuzhao, Analysis of driving fatigue factors and their mechanisms based on safety ergonomics Journal of Henan University of Technology (Natural Science Edition (1) (2008) 21–27, https://doi.org/10.16186/j.cnki.1673-9787.2008.01.017.

[26] Bi-Qin Zhang, Xiaoguang Chen, Feng Xu, Haiqiang Lei, Evaluation of Desert Highway Landscape, 2005. Highway and Transportation Science and Technology (S2).

[27] Shuo Zhang, Ji Xiaoqiang, Ge Yang, Chen Xuanru, Shi Lemin, Evaluation of psychological stress using a combination of electrocardiogram and EEG signals Journal of Changchun University of Science and Technology (Natural Science Edition) (2) (2020) 127–134.